

# Unsteady Trailing Vortex Evolution Behind a Wing in Ground Effect

Cheolheui Han\* and Jinsoo Cho†  
Hanyang University, Seoul 133-791, Republic of Korea

The unsteady evolution of trailing vortex sheets in ground effect is simulated by the use of a discrete vortex method. The ground effect is included by image method. Two cases of unsteady vortex evolution behind lifting lines (an elliptic loading and a fuselage/flap-wing configuration) are simulated for several ground heights. The present method is validated by comparison of the simulated wake roll-up shapes to published numerical results. For a lifting line with an elliptic loading, the ground has the effect of moving the wingtip vortices laterally outward and suppressing the development of the vortex. An increase in the wing loading has the effect of moving the wingtip vortex more laterally outward. The rotation of the wake vortices behind a fuselage/part-span flap configuration in ground effect is less than the case of flight out of the ground effect.

## Nomenclature

$b$	=	span
$C(\Gamma, t)$	=	point on a lifting line in the complex plane
$C'(\Gamma^o, t)$	=	point on an image lifting line in the complex plane
$h$	=	ground height; distance from a lifting line to the ground
$N$	=	number of point vortices
$R_e$	=	vortex Reynolds number
$r_c$	=	vortex core radius
$r_{c0}$	=	initial vortex core radius
$r_{ji}$	=	distance from the $i$ th point to the $j$ th point
$T$	=	total time, s
$t$	=	time, s
$u$	=	induced velocity in downstream direction
$v$	=	induced velocity in spanwise direction
$x$	=	distance in downstream direction
$y$	=	distance in spanwise direction
$z$	=	distance in vertical direction
$\bar{z}$	=	complex conjugate of $z$ in the complex plane
$\Gamma$	=	circulation of a lifting line
$\Gamma_j$	=	circulation of a vortex at the $j$ th point
$\Gamma^o$	=	circulation of an image lifting line
$\Gamma_0$	=	maximum circulation
$\gamma$	=	vortex sheet strength; distance between the origin of a vortex core to a point in space
$\Delta t_j$	=	growth age
$\delta$	=	smoothing factor
$\delta t$	=	time step
$\tau$	=	pseudotime

## Introduction

THE study of wing-in-ground effect (WIG) was initiated at the beginning of the 20th Century in relation to the takeoff and landing of aircraft. In recent years, there have been worldwide efforts to develop new conceptual vehicles focused on increasing efficiency and economy of shipping operation by exploitation of the WIG. Some of these vehicles have either been built or are under consideration. An important problem in the aerodynamic design of wing-in-ground effect vehicles (WIGV) is the accurate prediction

of the aerodynamic characteristics of a wing that is in close proximity to the ground. Numerous investigations have been conducted to understand this phenomenon and to develop the numerical aerodynamic analysis tools for the reliable prediction of the performance of the vehicle.<sup>1</sup>

Reference 2 discusses the difficulty of application of computational fluid dynamics to WIG aerodynamics. Panel methods have been frequently applied to the conceptual design of WIGV. The advantage of these methods is that they can be applied to the external aerodynamic problems of complex geometries with less effort than other numerical methods. Panel methods model the viscous shear layer behind the trailing edge of a wing as a vortex sheet. This approach is reasonable when the Reynolds number is infinite and the viscous shear layer is confined to a thin region. Many free-wake analysis techniques have been developed to obtain a reliable prediction of vortex flows for the analysis of fighter aircraft, missiles, and helicopters. Hoeijmakers and Vaatstra<sup>3</sup> have demonstrated the accuracy of a second-order panel method by showing the roll-up of a simulated wake behind various configurations, including an elliptically loaded wing, a ring wing, a fuselage/part-span flap/wing combination, and a delta wing. Ribeiro and Kroo<sup>4</sup> coupled the vortex-in-cell method with a vortex-lattice method through the use of a subvortex technique. Zhu and Takami<sup>5</sup> investigated the ground effect on vortex wake roll-up behind a lifting surface using a vortex-lattice method. However, the solution diverges when the wing is in close proximity to the ground. Lamarre and Paraschivoiu<sup>6</sup> presented a computational method to improve the accuracy of a three-dimensional low-order panel method using a two-dimensional unsteady analogy in the crossflow plane.

When a wing advances at a specified velocity, the shape of a two-dimensional vortex sheet resembles the shape of the cross section of the three-dimensional sheet at a distance behind the wing. Over the past few decades, a large number of attempts have been made to investigate the dynamics of the evolution of an unsteady two-dimensional vortex sheet to understand the large-scale behavior of the roll-up of the aircraft trailing vortices and their interactions with ambient shear. (See Sarpkaya<sup>7</sup> for a comprehensive review.)

Pullin<sup>8</sup> investigated the roll-up of an initially plane semi-infinite vortex sheet. He showed that, after a few iterations, the shape of the vortex sheet appears to be well approximated by Kaden's nearly circular asymptotic spirals. Krasny<sup>9</sup> showed that the numerical instability due to short-wavelength perturbations is a result of computer roundoff error. A filtering technique was used to suppress the growth of spurious roundoff error perturbations. Krasny<sup>10</sup> also desingularized the evolution equation using a smoothing parameter and demonstrated the exact vortex-sheet evolution at a fixed moderate time. Zabusky et al.<sup>11</sup> provided a means to investigate the evolution of inviscid flows with regions of vorticity by introducing a piecewise constant vorticity distribution.

Received 14 November 2003; revision received 30 March 2004; accepted for publication 30 March 2004. Copyright © 2004 by the American Institute of Aeronautics and Astronautics, Inc. All rights reserved. Copies of this paper may be made for personal or internal use, on condition that the copier pay the \$10.00 per-copy fee to the Copyright Clearance Center, Inc., 222 Rosewood Drive, Danvers, MA 01923; include the code 0021-8669/05 \$10.00 in correspondence with the CCC.

\*Graduate Student, School of Mechanical Engineering.

†Professor, School of Mechanical Engineering.

The interaction of aircraft trailing vortices with shear layers is inviscid in nature.<sup>12–14</sup> Therefore, Zheng and Baek<sup>15</sup> developed a vortex method to simulate the trajectory of wake vortices that interact with the shear layer. The computational efficiency of the vortex method was demonstrated in comparison with the Navier–Stokes numerical simulation. Morky<sup>16</sup> proposed a two-dimensional algorithm (based on a constant vortex sheet method) for modeling the evolution and propagation of aircraft trailing vortices in a shear flow that is near the ground. Robins et al.<sup>17</sup> developed an algorithm to predict the trajectories and decay in circulation of an aircraft's trailing vortices. Near the ground, where the viscosity plays an important role, they showed that the circulation decay for vortices appears to be independent of the ambient turbulence level. Darracq et al.<sup>18</sup> suggest that the effect of viscosity on the trajectories of the vortices and their interactions with shear layers at high Reynolds numbers is relatively minor. Benedict et al.<sup>19</sup> demonstrated that the numerical scheme of the wake roll-up is stable and correct when the thickness of the vortex sheet is nonzero. Therefore, the evolution of a trailing vortex in ground effect (IGE) may be examined using a thin vortex sheet in a discrete vortex method.

The objective of the present work is to develop a simple way of representing the evolution of vortices behind a WIG by the use of a discrete vortex method. In this approach, a lifting line with an initial load distribution is discretized with discrete vortex elements. The trailing wake vortices from each vortex element are represented by free vortices that can deform freely with an assumption of a force-free position.

### Discrete Vortex Method

The roll-up of a wake behind a finite span wing is a three-dimensional phenomenon. The problem of studying an unsteady two-dimensional curve in the crossflow plane is simplified when the rates of change of vorticity and geometry along the longitudinal (freestream) direction are small compared to the lateral (spanwise) direction. For a high aspect ratio ( $AR > 3$ ) wing that is at sufficiently low incidences angle of attack [AOA < 5 degrees], the unsteady evolution of the wake vortices from the trailing edge is similar to the time-dependent self-induced deformation of an infinitely long vortex sheet. The vortex-sheet approach that is used here is appropriate at very high Reynolds numbers because the wake vortices are then confined to a very thin region and the viscous effects are negligible outside of this region.

We follow the formulation of the roll-up of a vortex sheet as given by Birkhoff.<sup>20</sup> Consider a free vortex sheet that at time  $t < 0$  is stretched along the  $y$  axis; the lines of constant vorticity are perpendicular to the  $(y, z)$  plane. The vortex sheet behind the lifting surface is represented as a curve  $c(\Gamma, t) = y(\Gamma, t) + iz(\Gamma, t)$  in the complex plane. The circulation  $\Gamma$  is a Lagrangian parameter along the curve. The evolution equation for the vortex sheet is

$$\frac{\partial \bar{z}}{\partial t} = \frac{dW}{dc} \quad (1)$$

where the left-hand side is the Lagrangian velocity of a sheet fluid particle and the right-hand side is the Eulerian complex velocity field. Equation (1) represents the convection of a fluid particle at the local fluid velocity. For a vortex sheet with finite width, the complex velocity at an arbitrary point on the sheet is

$$\frac{dW}{dc} = \frac{1}{2\pi i} \oint_c \frac{d\Gamma^*}{[c(\Gamma, t) - c(\Gamma^*, t)]} + \frac{1}{2\pi i} \oint_c \frac{d\Gamma^o}{[c(\Gamma, t) - c'(\Gamma^o, t)]} \quad (2)$$

This integrodifferential equation yields the time-dependent velocity. The vortex sheet is represented as a series of straight-line segments (Fig. 1). Each segment is assumed to have a constant-strength vortex. This constant-strength vortex element is replaced by a single vortex with the same vorticity. On each line segment, a point vortex is located at the three-quarter point. In the case of a lifting line with elliptic loading, the circulation of the trailing horseshoe

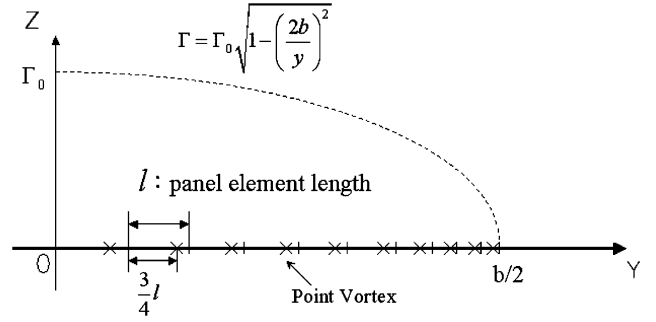


Fig. 1 Discrete vortex representation of a lifting line with elliptic loading.

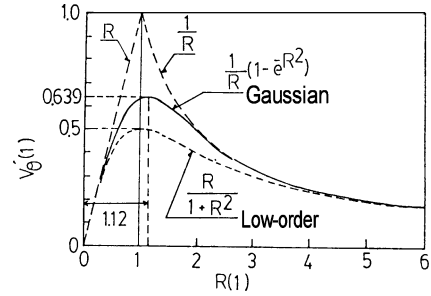


Fig. 2 Distributions of the dimensionless tangential velocities induced by a point vortex.<sup>19</sup>

vortices  $G(y)$  is

$$G(y) = -\frac{d\Gamma(y)}{dy} dy = \Gamma_0 y \left[ 1 - \left( \frac{2y}{b} \right)^2 \right]^{-\frac{1}{2}} dy \quad (3)$$

The velocity components that are induced at the point  $(y_j, z_j)$  by a point vortex of strength  $G_i$  that is located at  $y_i, z_i$  is

$$u = \frac{G_i(z_j - z_i)}{2\pi r_{ji}^2}, \quad v = -\frac{G_i(y_j - y_i)}{2\pi r_{ji}^2} \quad (4)$$

Because the complex number is a plane vector, Eq. (4) can be written as

$$\mathbf{w}_j = \frac{G_i}{2\pi} \sum_{i=1}^N \left[ \frac{(z_j - z_i)}{r_{ji}^2} \mathbf{i} - \frac{(y_j - y_i)}{r_{ji}^2} \mathbf{j} \right] \quad (5)$$

The distributions of the dimensionless tangential velocities induced by a point vortex are shown in Fig. 2. However, a real vortex is not a concentrated singularity of infinite vorticity. The more common models for a real vortex are the Rankine and the Lamb (Oseen) model (see Ref. 21). The Rankine vortex rotates as a solid body within a core. The Lamb model has a Gaussian distribution of vorticity. Ling et al.<sup>22</sup> proposed a model that is based on the solution for the actual velocity that is induced by a vortex in a viscous fluid. The core radius  $r_c$  is approximately equal to the radial distance of the point where the maximum velocity is induced. This is expressed<sup>23</sup>

$$r_{cj} = r_{cj0} + 3.17 \sqrt{\Delta t_j / R_e} \quad (6)$$

The second term on the right-hand side of Eq. (6) provides an estimate for the growth in the core radius of the vortex. The vortex Reynolds number is related to the timescale over which the laminar diffusion processes in the vortex core region become turbulent.<sup>23</sup> In the present work, an infinite Reynolds number is assumed. The velocity within the core ( $v_{\theta j}$ ) is

$$v_{\theta j} = (\Gamma_j / 2\pi r) \{ 1 - \exp[-1.25643(r/r_{cj})^2] \} \quad (7)$$

Outside the core region, the induced velocity is assumed to be that of a free vortex of strength  $\Gamma_j$ .

This vortex core model is strictly valid only for a single viscous vortex in an unbounded incompressible flow.<sup>23</sup> Vortex methods, therefore, use several smoothing schemes to remove the infinite energy that results from the point-vortex discretization of the equations. Reference 24 shows the problems of obtaining accurate solutions in the discretization of the Birkhoff–Rott equation. Krasny<sup>10</sup> avoids the singularity in the induced velocity of a point vortex through a smoothing factor,  $\delta$  (Ref. 10). The Eq. (5) can then

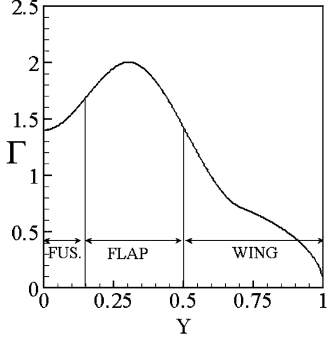
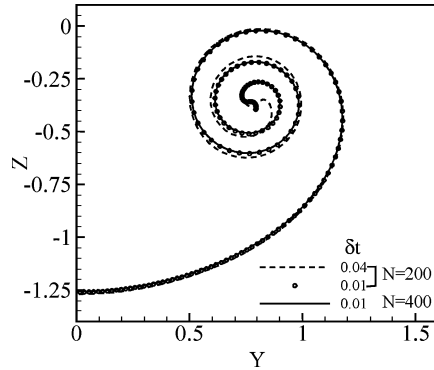
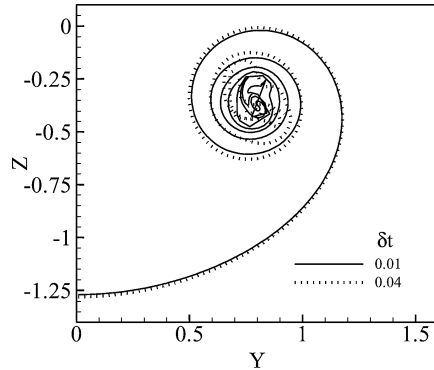


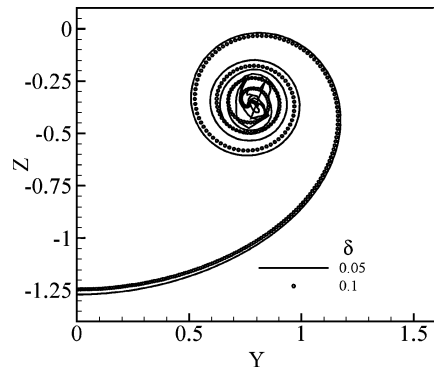
**Fig. 3 Fuselage/flap-wing, initial circulation distribution.**



**a) Gaussian smoothing ( $r_c = 0.15$ )**



**b) Low-order smoothing ( $N = 400$ ,  $\delta = 0.05$ )**



**c) Low-order smoothing ( $N = 400$ ,  $\delta t = 0.01$ )**

**Fig. 4 Comparison between two smoothing schemes ( $T = 4$  s).**

be written as follows

$$\mathbf{w}_j = \frac{G_i}{2\pi} \sum_{i=1}^N \left( \frac{(z_j - z_i)}{r_{ji}^2 + \delta^2} \mathbf{i} - \frac{(y_j - y_i)}{r_{ji}^2 + \delta^2} \mathbf{j} \right) \quad (8)$$

To enforce the no penetration condition at the ground, an image method is used. Because the wake is force-free, the evolution of each vortex is investigated by tracing the point vortices in pseudotime  $\tau$  and by moving the wake at the local flow velocity. The local flow velocity is the aggregate of the velocity components induced by all of the vortices. To determine the roll-up of the wake at each time, the induced velocity  $(u, v)_j$  at each vortex wake point  $j$  is calculated, and then the vortex elements are moved with an Euler convection scheme:

$$(\Delta y, \Delta z)_j = (u, v)_j \delta t \quad (9)$$

#### Wing with Elliptic Loading

In this case, the strength of the vortex sheet has algebraic singularities at  $y = \pm 1$ . On the horizontal axis,  $z = 0$ , the sheet's velocity becomes infinite as  $y \rightarrow 1$  from above and as  $y \rightarrow -1$  from below. It is commonly known that the two ends of the vortex sheet roll-up into counter-rotating spirals. The nonuniqueness of the solutions to this initial value problem has not yet been rigorously proven. However, the rolling up of the vortex sheet is known as the physically reasonable solution<sup>10</sup>:

$$\Gamma(y) = (1 - y^2)^{\frac{1}{2}}, \quad |y| < 1, \quad t = 0 \quad (10)$$

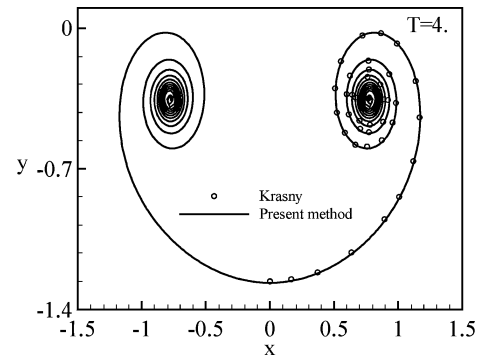
#### Fuselage/Flap-Wing

The initial distribution of the circulation for a fuselage/flap-wing configuration (as shown in Fig. 3) is

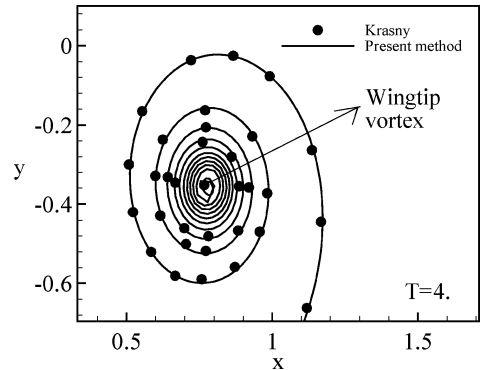
$$\Gamma(y) = a_1 y^3 + a_2 y^2 + a_3 y + a_4 y, \quad |y| \leq 0.3$$

$$\Gamma(y) = b_1 y^3 + b_2 y^2 + b_3 y + b_4 y, \quad 0.3 \leq |y| \leq 0.7$$

$$\Gamma(y) = (1 - y^2)^{\frac{1}{2}}, \quad 0.7 \leq |y| \leq 1.0 \quad (11)$$



**a) Rollup wake shape at  $T = 4.0$**



**b) Enlarged view near the wingtip vortex**

**Fig. 5 Comparison of the present method to the result of Krasny.<sup>10</sup>**

For  $|y| \leq 0.3$ , the coefficients of Eq. (17) are determined with the constraints:  $\Gamma(0) = 1.4$ ,  $\Gamma(0) = 0.$ ,  $\Gamma(0.3) = 2.0$ , and  $\Gamma(0.3) = 0$ . For  $0.3 \leq |y| \leq 0.7$ , the same data at  $y = 0.3$  are used together with the constraints:  $\Gamma(0.7) = (1 - 0.7^2)^{0.5}$  and  $\Gamma(0.7) = -0.7/(1 - 0.7^2)^{0.5}$ .

## Results and Discussions

One of the problems encountered by wake simulation programs that use potential flow theory is how to represent the roll-up of wake

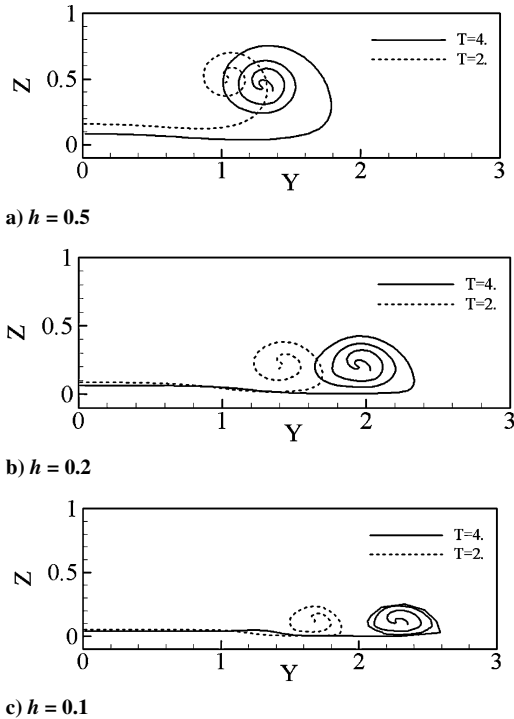


Fig. 6 Ground effect on the unsteady evolution of the vortex sheets ( $N = 200$ ,  $\delta t = 0.01$ ).

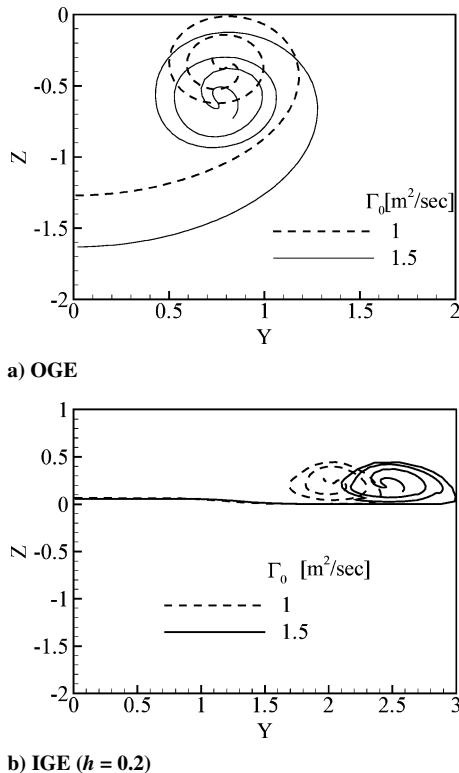


Fig. 7 Effect of wing loadings on wake rollup ( $T = 4$ ,  $N = 200$ ,  $\delta t = 0.01$ ).

vortices accurately in the highly rolled-up region without unrealistic vortex sheet crossings.<sup>3,4,5</sup> The case of an elliptically loaded wing is widely used to compare wake-modeling schemes.<sup>3,4</sup>

Figure 4 shows the computed wake shapes in the Trefftz plane at  $T = 4$  s. The computations are performed for a lifting line with elliptic loading. The effects of the smoothing factor, the time step, and the number of point vortices are investigated. The results found with a Gaussian smoothing scheme do not show instability in the core region of the vortex either with a small number of point vortices or at a large time step. However, a large number of turnings cannot be obtained with this scheme. In Fig. 4b, the effect of the time step is investigated for a low-order smoothing scheme. This scheme increases the number of turnings compared with the Gaussian smoothing scheme. However, unrealistic vortex sheet crossings due to a Kelvin–Helmholtz instability are observed shown even with a small time step of  $\delta t = 0.01$ . Figure 4c shows that when a larger smoothing factor of  $\delta = 0.1$  is used, it is possible to capture the roll-up of wake without unrealistic crossings of the vortex sheet.

In Fig. 5, the accuracy of the present method is validated by comparison of the wake shapes behind a lifting line having an elliptic

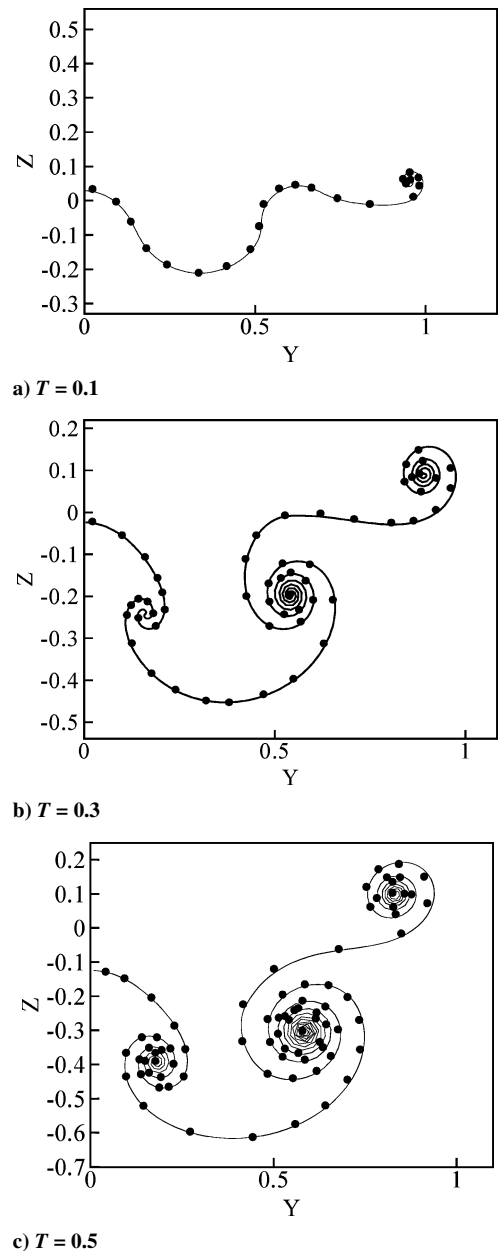


Fig. 8 Validation of simulated wake shapes for a fuselage/flap-wing configuration (OGE), Krasny<sup>10</sup>,  $N = 1000$ ,  $\delta = 0.02$ ,  $\delta t = 2 \times 10^{-3}$ ; solid line, — present method,  $N = 1000$ ,  $\delta = 0.02$ ,  $\delta t = 1.25 \times 10^{-3}$ .

loading with the published result of Krasny.<sup>10</sup> The in-flow velocity  $U$  and the maximum circulation  $\Gamma_0$  at the midspan are both assumed to be unity. The smoothing factor for the present calculation is set to 0.05 (the same as Krasny's). The smoothing factor has an effect of filtering the grid-scale noise and its choice for numerical simulation is usually based on machine precision.<sup>24</sup> To obtain a sufficient number of turnings, a time step of 0.0025 is used, which is four times smaller than that of Krasny.<sup>10</sup> It can be deduced from the Fig. 5 that the present results are in good agreement with Krasny's.<sup>10</sup>

It is known that the wake vortices behind a WIG cannot fully develop due to the insufficient distance between the wing and the ground. Thus, the strength of wingtip vortices is weaker compared to the case of wings out of ground effect. Figure 6 shows the ground effect on the unsteady evolution of the wake vortices behind a lifting line with elliptic loading. Because the lifting line is closer to the ground, the size of the core of the wingtip vortex is reduced, whereas the positions of the wingtip vortices are moved laterally more outward. The desingularized point vortices become confined

to a small region and coalesce. Thus, the total circulation decreases as the vortices evolve.

In Fig. 7, the effect of wing loading is investigated; it is assumed that the vortex strength increases proportionally with the aircraft's weight. Figure 7a shows the effect of the wing loading on the wake roll-up behavior behind a wing out of ground effect. The position of a tip vortex from the larger aircraft moves more downward compared with that of the smaller aircraft. It can be deduced from Fig. 7a that the bigger core size of the larger aircraft results in stronger tip vortex. Figure 7b shows the effect of wing loading on the wake roll-up behavior behind a WIG ( $h = 0.2$ ). The position of a tip vortex behind the wing with larger wing loading moves more laterally outward in the spanwise direction, whereas its position, from the ground, and size are similar to those of the wingtip vortex from the wing with smaller loading. It is known that, due to the viscous interaction between the vortices and the ground, a boundary layer develops as the vortices move downward. When the vortices are closer to the ground, the induced crossflow results in the detachment

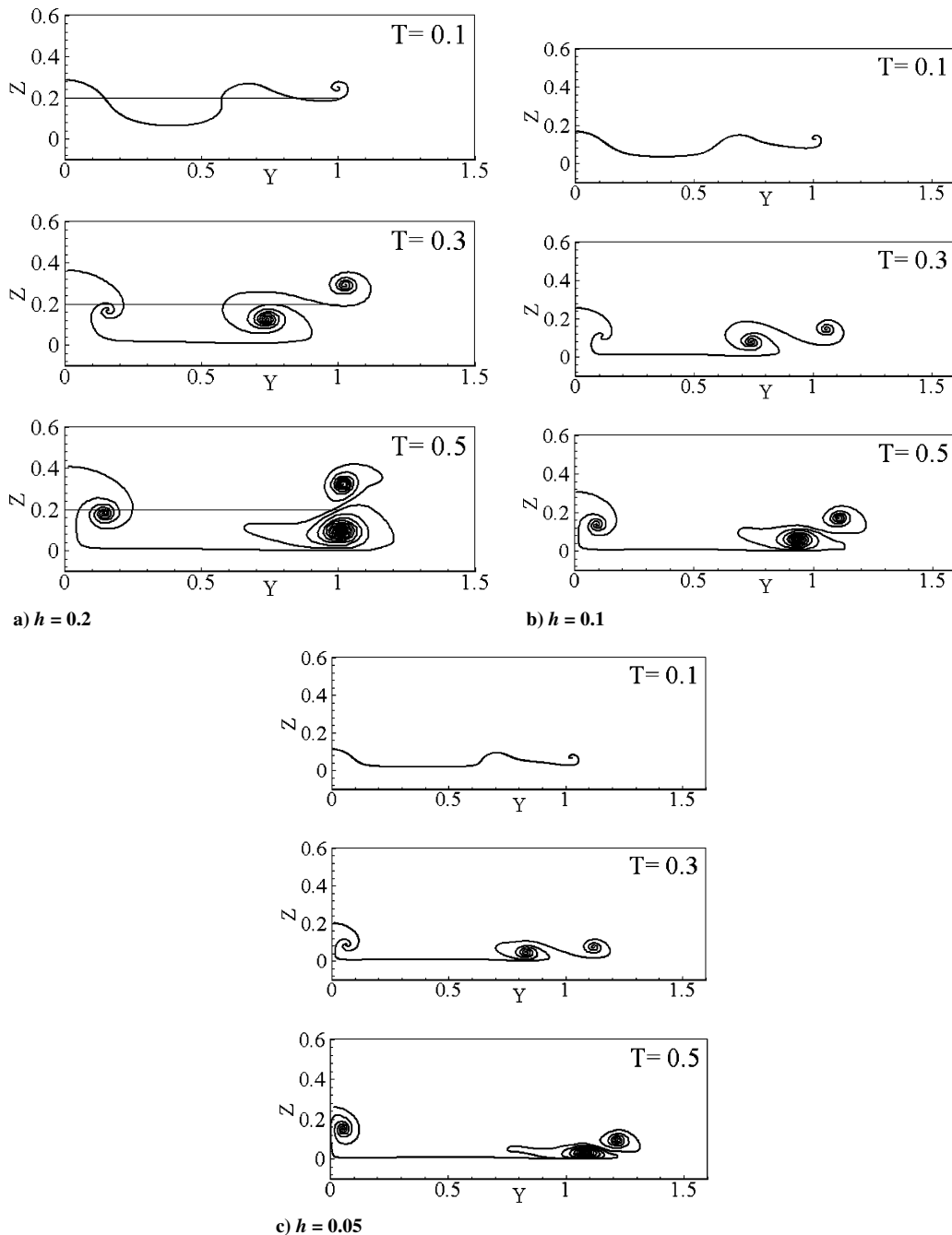


Fig. 9 Simulated wake roll-up for a fuselage/flap-wing configuration (IGE),  $N = 1000$ ,  $\delta = 0.02$ ,  $\delta t = 5.0 \times 10^{-4}$ .

of the boundary layer and the creation of a secondary vortex. The secondary vortex may interact with primary vortex.<sup>25,26</sup>

The modeling of the wake behind a complex configuration is important because of the possible adverse effects of the wake on control surfaces. Figure 8 shows the simulated wake roll-up behavior for a fuselage and part-span flap configuration out of ground effect. The present results show good agreement with Krasny's results.<sup>10</sup>

The ground effect on the wake behavior behind the fuselage-flap configuration is investigated next for several ground heights ( $h = 0.2, 0.1$ , and  $0.05$ ). A single-branched tip vortex and two spiral vortices (the flap vortex and the fuselage vortex) develop in the half-span region. The tip vortex first rolls up. Then, the flap vortex rolls up, and at a later time the fuselage vortex also rolls up. As shown in Fig. 8 in the out of ground effect (OGE) case, the tip vortex and the flap vortex rotate around each other because their circulations have the same sense of rotation. However, it is clearly shown in Fig. 9 that when a lifting line is in close proximity to the ground ( $h < 0.1$ ), the ground prevents the tip and flap vortices from rotating around each other. In Fig. 9, the flap vortex is observed to be the largest of the three vortices. The ground hinders the vortices from rolling up or rotating around each other, and, therefore, a weaker strength of the flap vortex results for the smaller ground height.

### Conclusions

In this paper, a discrete vortex method is developed to predict the wake behavior behind a WIG.

From the results, it is shown that a small time-step size and a moderate smoothing factor provide accurate solutions of the unsteady large-scale motion of wingtip vortices behind a lifting line with elliptic loading. For this lifting line with elliptic loading, the effect of proximity to the ground is to move the wingtip vortices laterally outward and to suppress the development of the vortices. The effect of wing loading is to move the wingtip vortex more downward for wings that are OGE. When the wing is IGE, the larger wing loading has the effect of moving the wingtip vortex more laterally outward. For the wake shapes behind a fuselage/part-span flap configuration, the proximity to the ground hinders the vortices from rotating around each other.

### Acknowledgment

This work was supported by the research fund of Hanyang University (HY-2002-I).

### References

- Rozhdestvensky, K. V., *Aerodynamics of a Lifting System in Extreme Ground Effect*, Springer-Verlag, Berlin, 2001, pp. 1–22.
- Larsson, L., Regnström, B., Broberg, L., Li, D.-Q., and Janson, C.-E., "Failures, Fantasies, and Feats in the Theoretical/Numerical Prediction of Ship Performance," *Proceedings of the Twenty-Second Symposium on Naval Hydrodynamics*, preprint, Washington, DC, Aug. 1998.
- Hoeijmakers, H. W. M., and Vaatstra, W., "A Higher Order Panel Method Applied to Vortex Sheet Roll-Up," *AIAA Journal*, Vol. 21, No. 4, 1983, pp. 516–523.
- Ribeiro, R. S., and Kroo, I., "Vortex-in-Cell Analysis of Wing Wake Roll-Up," *Journal of Aircraft*, Vol. 32, No. 5, 1995, pp. 962–969.
- Zhu, K., and Takami, H., "Effect of Ground on Wake Roll-Up Behind a Lifting Surface," *Proceedings of the 37th Japan National Congress for Applied Mechanics*, Vol. 37, 1987, pp. 115–123.
- Lamarre, F., and Paraschivoiu, I., "Efficient Panel Method for Vortex Sheet Roll-Up," *Journal of Aircraft*, Vol. 29, No. 1, 1992, pp. 28–33.
- Sarpkaya, T., "Computational Methods With Vortices—The 1988 Freeman Scholar Lecture," *Journal of Fluids Engineering*, Vol. 111, No. 1, March 1989, pp. 5–52.
- Pullin, D. I., "The Large-Scale Structure of Unsteady Self-Similar Rolled-up Vortex Sheets," *Journal of Fluid Mechanics*, Vol. 88, Pt. 3, 1978, pp. 401–430.
- Krasny, R., "A Study of Singularity Formation in a Vortex Sheet by the Point-Vortex Approximation," *Journal of Fluid Mechanics*, Vol. 167, 1986, pp. 65–93.
- Krasny, R., "Computation of Vortex Sheet Roll-up in the Trefftz Plane," *Journal of Fluid Mechanics*, Vol. 184, 1987, pp. 123–155.
- Zabusky, N. J., Hughes, M., and Roberts, K. V., "Contour Dynamics for the Euler Equations In Two Dimensions," *Journal of Computational Physics*, Vol. 30, No. 96, 1979, pp. 96–106.
- Campbell, S. D., Dasey, T. J., Freehart, R. E., Heinrichs, R. M., Matthews, M. P., and Perras, G. H., "Wake Vortex Field Measurement Program at Memphis, TN," AIAA Paper 96-0399, Jan. 1996.
- Proctor, F. H., Hinton, D. A., Han, J., Schowalter, D. G., and Lin, Y. L., "Two Dimensional Wake Vortex Simulation in the Atmosphere: Preliminary Sensitivity Studies," AIAA Paper 97-0056, Jan. 1997.
- Proctor, F. H., "The NASA-Langley Wake Vortex Modeling Effort in Support of an Operational Aircraft Spacing," AIAA Paper 98-0589, Jan. 1998.
- Zheng, Z. C., and Baek, K., "Inviscid Interactions Between Wake Vortices and Shear Layers," *Journal of Aircraft*, Vol. 36, No. 2, 1999, pp. 477–480.
- Morky, M., "Numerical Simulation of Aircraft Trailing Vortices Interacting with Ambient Shear or Ground," *Journal of Aircraft*, Vol. 38, No. 4, 2001, pp. 636–643.
- Robins, R. E., Delisi, D. P., and Greene, G. C., "Algorithm for Prediction of Trailing Vortex Evolution," *Journal of Aircraft*, Vol. 38, No. 5, 2001, pp. 911–917.
- Darracq, D., Moet, H., and Corjon, A., "Effect of Crosswind Shear and Atmospheric Stratification on Aircraft Trailing Vortices," AIAA Paper 99-0985, Jan. 1999.
- Benedict, K., Kornev, N., Meyer, M., and Ebert, J., "Complex Mathematical Model of the WIG Motion Including the Take-off Mode," *Ocean Engineering*, Vol. 29, No. 3, 2002, pp. 315–357.
- Birkhoff, G., "Helmholz and Taylor Instability," *Proceeding of Symposium on Applied Mathematics*, Vol. 13, 1962, pp. 55–76.
- Ogawa, A., *Vortex Flow—CRC Series on Fine Particle Science and Technology*, CRC Press, Boca Raton, FL, 1940.
- Ling, G. C., Bearman, P. W., and Graham, J. M. R., "A Further Simulation of Starting Flow Around a Flat Plate by a Discrete Vortex Model," *Internal Seminar on Engineering Applications of the Surface and Cloud Vorticity Methods*, Vol. 51, No. 14, 1986, pp. 118–138.
- Leishman, J. G., *Principles of Helicopter Aerodynamics*, Cambridge Univ. Press, Cambridge, England, U.K., 2000, pp. 435–443.
- Majda, A. J., and Bertozzi, A. L., *Vorticity and Incompressible Flow*, Cambridge Univ. Press, Cambridge, England, U.K., 2002, pp. 359–382.
- Corjon, A., and Poinot, T., "Wake Vortices Behavior Near the Ground," *European Series in Applied and Industrial Mathematics Proceedings*, Vol. 1, No. 20, 1996, pp. 279–294.
- Moet, H., Laporte, F., Darracq, D., and Corjon, A., "Investigation of Ambient Turbulence on Vortex Evolution Using LES," AIAA Paper 2000-0756, 2000.